



ELSEVIER

Available online at www.sciencedirect.com



Optics Communications xxx (2002) xxx–xxx

OPTICS
COMMUNICATIONS

www.elsevier.com/locate/optcom

2 Phase retrieval by demodulation of a Hartmann–Shack sensor

3 Yuval Carmon^{a,b}, Erez N. Ribak^{a,*}

4 ^a *Department of Physics, Technion, Haifa 32000, Israel*

5 ^b *Shamir Optical Industries, Shamir, Upper Galilee 12135, Israel*

6 Received 11 July 2002; received in revised form 6 November 2002; accepted 1 December 2002

7 Abstract

8 We develop a method for retrieving the wavefront from a Hartmann–Shack sensor using a two-dimensional Fourier
9 demodulation technique. This provides a means for analyzing the patterns produced by a Hartmann–Shack sensor with
10 variable lenslet array pitch. The technique is based on applying a digital demodulation technique twice on the pattern,
11 along two orthogonal axes. This provides both phase gradient components in real space. Later a Laplacian Fourier
12 reconstruction is used to obtain the corresponding wavefront. We discuss the robustness of the technique to Poisson
13 and white noise. Wavefront measurements of known aberrations are analyzed using this technique.
14 © 2002 Published by Elsevier Science B.V.

15 *PACS:* 07.05.Kf; 42.15.Dp; 42.30.Rx; 42.68.Wt

16 *Keywords:* Wavefront sensing; Hartmann–Shack sensor; Digital demodulation

17 In a Hartmann–Shack sensor [1], a wavefront
18 passes through a rigidly spaced lenslet array. The
19 displacement of the foci is sampled at the focal
20 plane of the lenslet array with relation to the center
21 of sub-aperture of the respective lenslet. It is di-
22 rectly proportional to the average of the wavefront
23 gradient over the aperture. Thus the data extracted
24 from a measurement is the phase gradient field
25 sampled at discrete locations dictated by the lenslet
26 array. The common method today for extracting
27 this information is the centroiding method [2,3].

We suggest an alternative approach: Fourier de- 28
modulation. 29

Takeda and Mutoh [4] uses a one-dimensional 30
Fourier method to calculate the fringe phase. 31
Roddier et al. [5] describe a method for acquiring 32
the two-dimensional (2D) phase and amplitude of 33
a fringe visibility function; however, the fringes in 34
this case only provide information orthogonal to 35
the intensity contours. We offer a method for using 36
the 2D fast Fourier transform (FFT) twice, for 37
acquiring both gradient field components from a 38
Hartmann–Shack measurement. 39

We start by writing the expression for the irra- 40
diance function of the Hartmann–Shack pattern. 41
In this wavefront sensor, the dislocations of the 42
foci can be viewed as modulation of the foci grid. 43

*Corresponding author. Tel.: +972-4-829-2776; fax: +972-4-822-1514.

E-mail address: phr22er@technion.ac.il (E.N. Ribak).

44 Since this modulation is proportional to the phase
45 gradient, the main harmony of the spot pattern
46 intensity function is

$$I(\mathbf{r}) = V(\mathbf{r})\{2 - \cos[k_x x - F\phi_x] - \cos[k_y y - F\phi_y]\},$$

48 where $V(\mathbf{r})$ is the pattern amplitude at location
49 $\mathbf{r} = (x, y)$, and is assumed to be constant within the
50 optical aperture, without zero. k_x and k_y are the
51 two \mathbf{k} vector components: $k_x = 2\pi/P_x$ and
52 $k_y = 2\pi/P_y$, where the lenslet array pitch is $P_x \times P_y$.
53 F is the lenslet array focal length, and ϕ_x, ϕ_y are
54 the phase x and y derivatives at \mathbf{r} and are to be
55 determined. We can write this expression in the
56 following way:

$$I(\mathbf{r}) = 1/2\{2V(\mathbf{r}) - C_x(\mathbf{r})e^{ik_x x} - C_x^*(\mathbf{r})e^{-ik_x x} \\ - C_y(\mathbf{r})e^{ik_y y} - C_y^*(\mathbf{r})e^{-ik_y y}\}; \quad (1)$$

$$C_x(\mathbf{r}) = V(\mathbf{r})e^{-iF\phi_x},$$

$$C_y(\mathbf{r}) = V(\mathbf{r})e^{-iF\phi_y}.$$

58 The superscript asterisk * denotes a complex con-
59 jugate. Taking the Fourier transform of this ex-
60 pression we have

$$\hat{I} = \frac{1}{2}\{4\hat{V} - \hat{C}_x * \delta(q_x - k_x) - \hat{C}_x^* * \delta(q_x + k_x) \\ - \hat{C}_y * \delta(q_y - k_y) - \hat{C}_y^* * \delta(q_y + k_y)\} \\ = \frac{1}{2}\{4\hat{V}(q_x, q_y) - \hat{C}_x(q_x + k_x, q_y) - \hat{C}_x^*(q_x - k_x, q_y) \\ - \hat{C}_y(q_x, q_y + k_y) - \hat{C}_y^*(q_x, q_y - k_y)\}, \quad (2)$$

62 where * denotes a convolution and $\hat{\cdot}$ denotes the
63 Fourier transform. \hat{V} is non-zero only in a very
64 small area around the origin in Fourier Space.

65 It is assumed that the wavefront slope is
66 adiabatic: it is very slow compared with the
67 lenslet spatial frequency. This is a less restrictive
68 condition than that imposed by the commonly
69 used centroiding technique, where no spot is al-
70 lowed to stray outside its designated domain.
71 Adding the conditions for the two slopes, we
72 have

$$\nabla^2 \phi(\mathbf{x}) \ll \nabla(\mathbf{k} \cdot \mathbf{x})/F. \quad (3)$$

74 In other words, the *curvature* of the wavefront is
76 limited by the lenslet array pitch and focal length.
77 The adiabatic condition also means that the
78 typical frequency of the phase derivatives is much
79 smaller than the driver (lenslet) frequency.

Therefore, $C_x(\mathbf{r})$ and $C_y(\mathbf{r})$ have a cutoff frequency 80
 q_{cutoff} that is much smaller than the lenslet fre- 81
quency. From (2) \hat{I} is the sum of five isolated 82
lobes in Fourier space: $\hat{V}(q_x, q_y)$, $\hat{C}_x(q_x + k_x, q_y)$, 83
 $\hat{C}_x^*(q_x - k_x, q_y)$, $\hat{C}_y(q_x, q_y + k_y)$, $\hat{C}_y^*(q_x, q_y - k_y)$. The 84
demodulation process now proceeds in two steps. 85
The first is making a rigid translation (demodu- 86
lation) in Fourier space of magnitude $-q_x \hat{\mathbf{x}}$ to (2) 87
to eliminate the lenslet frequency along the x -axis 88
of the lobe $\hat{C}_x^*(q_x - k_x)$. The second is applying a 89
low pass filter with a cutoff frequency of q_{cutoff} , so 90
that information from the other lobes will not 91
seep in. After these two steps we are left with the 92
Fourier transform of $C_x(\mathbf{r})$. The *argument* of the 93
inverse Fourier of this expression from (1) is $F\phi_x$. 94
Applying a similar algorithm, but this time de- 95
modulating along the y -axis, we obtain $F\phi_y$. 96

The process is thus comprised of the following 97
steps: (1) zero-pad the image to twice the aperture 98
size; (2) Fourier transform the image; (3) multiply 99
the transform by a band-pass filter around the x 100
sidelobe; (4) center the result to the Fourier origin; 101
(5) inverse transform the filtered x lobe; (6) extract 102
the phase of the result, to yield the x slope of the 103
wavefront; (7–10) repeat (3–6) for the y lobe; (11) 104
reconstruct the phase from its x and y slopes. 105

In the centroiding method, in order to calculate 106
the displacement of the foci, the center of intensity 107
within each lenslet aperture is measured. The situ- 108
ation becomes more complicated if the wavefront 109
slope is too large and the correlating light spot 110
strays out of the designated lenslet sub-aperture. 111
Pfund et al. [6] offer a modified unwrapping 112
method for overcoming this problem, and Gro- 113
ening et al. [7] offer a method that uses extrapo- 114
lation with an iterative spline algorithm. In our 115
own method, this obstacle is dealt with automati- 116
cally since there is no rigid sub-aperture in which 117
the foci need fit. 118

The only restriction our method imposes is that 119
the generating wave front be a well-behaved 120
function, and that its cutoff frequency be sub- 121
stantially lower than the lenslet frequency. This 122
makes the dynamic range of the algorithm larger. 123
No a-priori information concerning the lenslet 124
array pitch needs to be provided. It is calculated 125
on the fly. The calculation is not seriously effected 126
if a small portion of the spots strays out of the 127

128 CCD detector altogether. Therefore, the restric-
129 tions imposed on the Hartmann sensor hardware
130 and experimental system configuration can be re-
131 laxated. If the aberrations do not meet condition (3),
132 we need to only use a higher modulating fre-
133 quency, with a denser lenslet array. A convenient
134 wavefront sensor is a flexible-pitch acoustic cell [8],
135 in which the lenslet period is easily varied. The
136 advantages of this method can be used when one
137 wants to measure phenomena that have a varying
138 spatial and temporal frequency, such as the aber-
139 rations induced by the atmosphere in astronomy,
140 or measurements of ocular aberrations, in which
141 there is a large variability in aberrations between
142 subjects.

143 The phase derivatives in (1) obtained using our
144 method, being arguments of exponential functions,
145 may be wrapped. It is desirable to compute the
146 unwrapped phase. The easiest way to set about
147 doing this is to sum the phase differences sampled
148 at discrete locations. This method suffices as long
149 as the differences are no larger than π . More
150 complex algorithms [9] have been devised to deal
151 with the circumstances in which this condition
152 does not apply.

153 Finally, equipped with the gradient field, we
154 need to calculate the generating wavefront. Tech-
155 niques for deducing the wavefront from the phase
156 gradient include zonal and modal fitting of the
157 phase to the gradient information [10–12]. Roddier
158 [5] offers a method for reconstructing the wave-
159 front using the FFT of its Laplacian. Since we deal
160 with demodulating the Hartmann patterns in
161 Fourier space, we thought it fitting to use this
162 method. It is based on the following observation: if
163 f is any function on which a Fourier transform
164 can be applied, then the following equality holds:

$$\Im[\partial_{x_j}^{(n)} f(\bar{x})] = i^n q_j^n \Im[f(\bar{x})], \quad (4)$$

166 where $\partial_{x_j}^{(n)}$ denotes the n th derivative with respect
167 to coordinate x_j , and q_j is the corresponding
168 Fourier coordinate. \Im denotes the Fourier trans-
169 form operator. Using (4), the Fourier transform of
170 the phase is

$$\Im[f(\bar{x})] = -(iq_x \Im[\partial_x f(\bar{x})] + iq_y \Im[\partial_y f(\bar{x})]) / (q_x^2 + q_y^2).$$

172 It is therefore seen that to calculate the phase, a
173 Fourier transform must be applied on each of the

174 phase derivatives computed in the previous step.
175 The technique that Roddier describes also includes
176 iterative imposition of the boundary conditions.
177 We have found that imposing periodic boundary
178 conditions changes the results only slightly, and
179 only at the edges.

180 We simulated the method: a random wavefront
181 that conforms to conditions (3) was generated on
182 the computer, and a correlating Hartmann pattern
183 computed. The phase was then reconstructed ac-
184 cording to the above-described algorithm. Since no
185 reference image was used for the simulation, we
186 removed the tip-tilt terms from the input and
187 output phases. In Fig. 1, we chose very large ex-

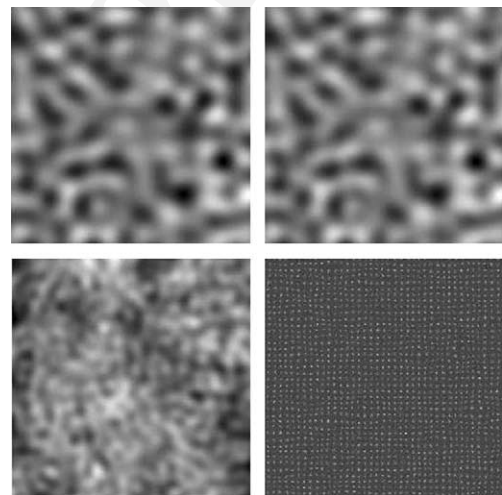


Fig. 1. Top left is the input phase 400×400 pixels, 4π peak to valley. We used a random phase, and applied a low pass filter with a cutoff frequency of 10 pixels. Bottom right shows the generated Hartmann-Shack pattern, which has added Poisson white noise with SNR = 1. Top right is the reconstructed phase. Bottom left is the phase difference between the input and output phases. The scale ratio between the phase maps and the difference map is 6.3, and the RMS of the difference is 0.25.

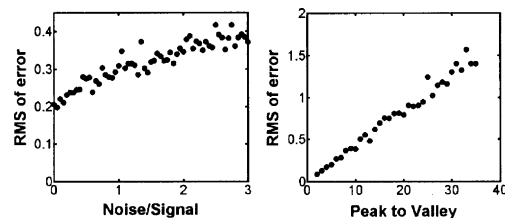


Fig. 2. Computation error grows linearly with the noise content (left) and the aberration content in radians (right).

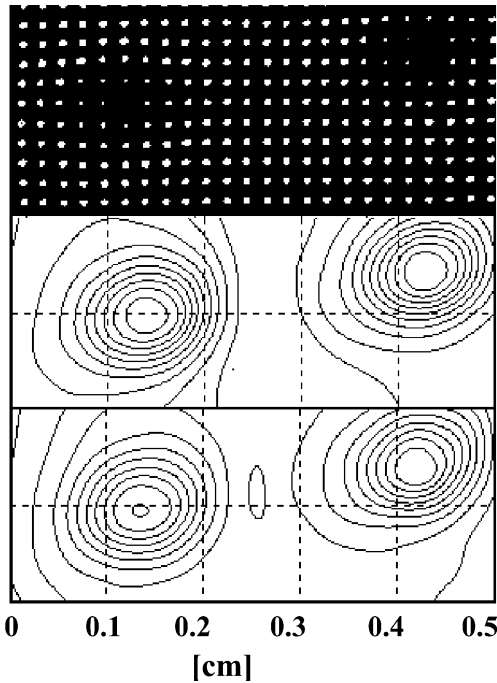


Fig. 3. The top measurement was taken with a lenslet array with diameters of 0.19 mm, and the bottom one with 0.25 mm. Contour gaps are 12 nm.

188 cursions from the wavefront (peak to valley of 4π)
189 and a large noise factor (SNR = 1). For this reason
190 the result differed from the input by a maximum of
191 0.08π .

192 Two more series of simulations were carried out
193 (Fig. 2). In the first, the noise to signal ratio was

increased, and mapped against the RMS error of 194
the computation. In the second, the mean aberration 195
was increased, and then mapped against the 196
RMS error of the computation. 197

Finally, we compared two actual measurements 198
with two different lenslet arrays of known aberrations. 199
The difference between the two results and 200
between each result and the known sample was of 201
a few percent. Residual tip, tilt and defocus errors 202
were left because the demodulation was done on 203
integer pixels. This constitutes most of the error 204
(see Fig. 3). 205

References

206

- [1] I. Ghozeil, in: D. Malacara (Ed.), Optical Shop Testing, 207
Wiley, New York, 1978 (Chapter 10). 208
- [2] R.K. Tyson, Principles Of Adaptive Optics, second ed., 209
Academic Press, New York, 1998. 210
- [3] R.K. Tyson (Ed.), Adaptive Optics Engineering Hand- 211
book, Marcel Decker, New York, 2000. 212
- [4] M. Takeda, K. Mutoh, Appl. Opt. 22 (1983) 3977. 213
- [5] F. and C. Roddier, Appl. Opt. 26 (1987) 1668. 214
- [6] J. Pfund, N. Lindlein, J. Schwider, Opt. Lett. 23 (1998) 995. 215
- [7] S. Groening, B. Sick, K. Donner, J. Pfund, N. Lindlein, J. 216
Schwider, Appl. Opt. 39 (2000) 561. 217
- [8] E.N. Ribak, Opt. Lett. 26 (2001) 1834. 218
- [9] D.C. Ghiglia, M.D. Pritt, Two-Dimensional Phase Un- 219
wrapping: Theory, Algorithms, and Software, Wiley-Inter- 220
science, New York, 1998. 221
- [10] R.H. Hudgin, J. Opt. Soc. Am. 67 (1977) 375. 222
- [11] D.L. Fried, J. Opt. Soc. Am. 67 (1977) 370. 223
- [12] W.H. Southwell, J. Opt. Soc. Am. 70 (1980) 998. 224